Original Article

Physoxia alters human mesenchymal stem cell secretome

Journal of Tissue Engineering
Volume 12: 1–14

DOI: 10.1177/20417314211056132
journals.sagepub.com/home/tej
SAGE

Marwan M Merkhan[1,2], Matthew T Shephard[1] and Nicholas R Forsyth[1]

Abstract

The human mesenchymal stem cell (hMSC) secretome has pleiotropic effects which underpin their therapeutic potential. hMSC serum-free conditioned media (SFCM) has been determined to contain a variety of cytokines with roles in regeneration and suppression of inflammation. Physiological oxygen (physoxia) has been demonstrated to impact upon a number of facets of hMSC biology and we hypothesized that the secretome would be similarly modified. We tested a range of oxygen conditions; 21% O_2 (air oxygen (AO)), 2% O_2 (intermittent hypoxia (IH)) and 2% O_2 Workstation (physoxia (P)) to evaluate their effect on hMSC secretome profiles. Total protein content of secretome was upregulated in IH and P (>3 fold vs AO) and IH (>1 fold vs P). Focused cytokine profiling indicated global upregulation in IH of all 31 biomolecules tested in comparison to AO and P with basic-nerve growth factor (bNGF) and granulocyte colony-stimulating factor (GCSF) (>3 fold vs AO) and bNGF and Rantes (>3 fold vs P) of note. Similarly, upregulation of interferon gamma-induced protein 10 (IP10) was noted in P (>3 fold vs AO). Interleukin-2 (IL2) and Rantes (in AO and P) and adiponectin, IL17a, and epidermal growth factor (EGF) (in AO only) were entirely absent or below detection limits. Quantitative analysis validated the pattern of IH-induced upregulation in vascular endothelial growth factor (VEGF), placental growth factor-1 (PIGF1), Tumor necrosis factor alpha (TNFa), IL2, IL4, and IL10 when compared to AO and P. In summary, modulation of environmental oxygen alters both secretome concentration and composition. This consideration will likely impact on delivering improved mechanistic understanding and potency effects of hMSC-based therapeutics.

Keywords

Secretome, mesenchymal stem cell, physoxia

Date received: 8 April 2021; accepted: 12 October 2021

Introduction

Mesenchymal stem cells (MSCs), first identified approximately 50 years ago, have a growing role in regenerative medicine as a treatment for various diseases and disorders.[1–3] The precise mechanisms of action remain unclear though likely related to all or a combination of the following; multipotent differentiation, functional incorporation, immunomodulation, and secretion of paracrine factors.[1,4,5] Proteomic profiling of serum-free conditioned media (SFCM) from human MSCs (hMSCs) have revealed the presence of a range of pleiotropic biomolecules within the secretome including vascular endothelial growth factor (VEGF), granulocyte-macrophage colony-stimulating factor (GMCSF), interleukin-10 (IL10), and leptin.[6–9] However, precise SFCM composition can vary, confusing interpretation where variations can result from hMSC source; for example, adipose tissue,[10] cord blood,[11,12] bone marrow aspirate,[13–15]stem cell lines [16]; culture conditions, conditioning periods, and classical monolayer versus 3D conditioning methods.[17]

Various in vitro studies have reported beneficial effects of hMSC SFCM supporting the paracrine hypothesis of

[1]Guy Hilton Research Centre, School of Pharmacy and Bioengineering, Keele University, Staffordshire, UK
[2]College of Pharmacy, University of Mosul, Mosul, Iraq

Corresponding author:
Matthew T Shephard, Guy Hilton Research Centre, School of Pharmacy and Bioengineering, Keele University, Staffordshire ST4 7QB, UK.
Email: m.t.shephard@keele.ac.uk

the regenerative potential of hMSCs. For instance, conditioned media (CM) promoted proliferation and migration of alveolar epithelial cells facilitating in vitro wound closure.[18–21] SFCM displayed beneficial effects in a Balb/C mouse model of excisional wound injury via increased deposition of regulatory macrophages and endothelial progenitor cells at the site of injury.[22] Additionally, there was improved functional recovery following hindlimb injury, induced by femoral artery ligation, via increased collateral angiogenesis and limb remodelling.[23] Moreover, it has been reported that intravenous infusion of SFCM promoted regeneration and inhibited cellular damage in a rat model of gentamicin-induced liver injury through accelerated proliferation and inhibition of apoptosis.[24] Further, localized administration of SFCM in a rat ischemic retinal model restored functionality via inhibition of retinal cell apoptosis and attenuation of ischemic effects.[25] More recently, studies have shown that CM produced under low oxygen culture conditions protects against ischemic stroke in rats and promotes angiogenesis through increased quantities of growth factors present, further adding to the body of evidence concerning the clinical application of these cell-free therapies.[9,26] Collectively, these confirm that SFCM may become a milestone therapeutic tool or a source for discovery of new bioactive therapeutic molecules.

The role of oxygen in stem cell biology has been described variously.[27–30] Physoxia is an inherent feature of the in vivo niche environment in which hMSCs are resident, drawing largely from the sinusoidal blood network characteristic of bone marrow.[31–33] Studies to define the pO_2 of in vivo environments, specifically sinusoidal bone marrow, have shown an average value of 2.7%.[34] Physoxia is significantly lower than inhaled air (21% O_2) and it declines gradually as it passes from the lung to the tissues; ranging between 0.1% and 9% with an average of 2% O_2.[33,35,36] It is also important to note that the journey of a transplanted stem cell from donor to recipient can be broadly divided into in vitro and in vivo stages. The in vitro stage features isolation and expansion under non-physiological conditions while the in vivo stage includes both donor (before isolation) and recipient (after transplantation) physiological environments.[35] The immediate physiological environment of the recipient will vary according to the preferred delivery method but focusing on one currently applied intravenous delivery methodology, the hMSC dose arrives into the physoxic blood stream having previously experienced a long-term association with air oxygen.[37,38]

Applying an increasingly in vivo-like physoxia to in vitro hMSC culture modulates the transcriptome and increasing evidence suggests this manifests itself via an altered secretome composition.[26,39–41] An altered secretome would likely impact on the reparative action of SFCM and would likely better reflect the behavior of hMSCs and/or their secretome following transplant into in vivo tissues. A range of control parameters can be applied to mimic conditions both before isolation and after transplantation, drawing comparisons to standard in vitro culture conditions. Therefore, this study sought to exploit available technologies to explore the role of different oxygen tensions on the secretome composition of hMSCs using air oxygen (AO) versus both intermittent hypoxia (IH) and physoxia (P) models. To the best of our knowledge, this study provides a first description of modulation of hMSC paracrine components linked to a physoxic or intermittent hypoxic setting.

Materials and methods

Cell culture

hMSCs were isolated and expanded from human bone marrow aspirate (BMA) using an adherence-based methodology.[39] A total of three samples of human BMA from three different donors (two male and one female, ages 20–36) were purchased from Lonza, USA and each seeded at a density of 1×10^5 mononuclear cells/cm^2 on fibronectin pre-coated culture flasks in Dulbecco's Modified Eagle Medium (DMEM) supplemented with 5% (v/v) fetal bovine serum (FBS), 1% (v/v) L-glutamine, 1% (v/v) non-essential amino acids (NEAA), and 1% (v/v) Penicillin-Streptomycin-Amphotericin B (PSA) (Lonza, UK). Seeded flasks were incubated in either a humidified incubator with a distinct oxygen tension (21% O_2 (AO), 2% O_2 (IH)) or in an oxygen control workstation (Baker Ruskinn, UK) (2% O_2 (P)). After 7 days, half of the media volume was removed and replaced with fresh antibiotic-free growth medium followed by a complete media change after a further 7 days. Media was then changed every 3 days until confluent. Once confluent, hMSC were enzymatically passaged with 1% Trypsin/EDTA (Lonza, UK) at 1:2 split ratios. Passage one (P1) cells and their CM were used for all experiments except for the transcriptome analysis which was performed with cells from a previously recorded dataset at P0.

SFCM was prepared by washing 70% confluent T75 flasks with phosphate-buffered saline (PBS) followed by 15 ml serum-free non-conditioned media (SFNCM) consisting of DMEM supplemented with 1% (v/v) L-glutamine and 1% (v/v) NEAA. For conditioning, 20ml of SFNCM was added to hMSC cultures and incubated for 24 h in their respective AO, IH, or P conditions. Following conditioning media was collected, centrifuged for 10 min at 300*g* and stored at −80°C as SFCM. Prior to use SFCM was thawed and filtered (0.2 μm). All SFCM was produced from hMSCs at P1. Time taken for hMSC isolation from BMA plating, expansion, passaging and reaching confluence at P1 was 28–29 days (28 days for donors 1 and 2, 29 days for donor 3) and was consistent between the three oxygen concentrations.

Flow cytometry

Immunophenotyping of hMSCs was performed using human PE-conjugated monoclonal antibodies (Miltenyi Biotech, UK) specific for CD14 (clone: Tük4/ catalog No.130-113-709), CD19 (clone: LT19/ catalog No. 130-113-731), CD34 (clone: AC136/catalog No. 130-113-741), CD45 (clone: 5B1/catalog No. 130-113-680), CD73 (clone: AD2/catalog No. 130-097-943), CD90 (clone: DG3/catalog No. 130-117-537), CD105 (clone: 43A4E1/ catalog No. 130-098-906), HLA-DR (clone: AC122/catalog No. 130-098-177). Mouse IgG_1 (clone: IS5-21F5/catalog No. 130-113-762) and IgG_{2a} (clone: S43.10/catalog No. 130-113-834) were used for isotype controls. Briefly, 1×10^5 hMSCs were aliquoted into individual microcentrifuge tubes, washed with incubation buffer (0.075% EDTA/0.5% BSA in PBS) and centrifuged for 5 min at 300*g*. Cell pellets were re-suspended in 100 µl of specific antibody solution followed by incubation at 4°C for 10 min. Labeled hMSCs were washed in a 10× volume of incubation buffer and centrifuged at 300*g* for 10 min. The supernatant was aspirated and cell pellets re-suspended in 200 µl incubation buffer for analysis on a Cytomic FC500 flow cytometer (Beckman Coulter, UK) and Cyflogic v.1.2.1(CyFlo Ltd, UK).

Trilineage differentiation

To confirm the differentiation potential of hMSCs, 2.5×10^4 cells/cm^2 were seeded overnight in DMEM supplemented media. Following overnight incubation, hMSC cultures were switched into differentiation media directed toward: osteogenesis (media supplemented with 50 µM ascorbic acid, 10 mM beta-glycerophosphate and 0.1 µM dexamethasone (Sigma, UK)); adipogenesis (media supplemented with 0.5 µM dexamethasone, 0.5 mM 3-isobutyl-1-methylxanthine, 1 µg/ml insulin and 100 µM indomethacin (Sigma, UK)); chondrogenesis (media supplemented with 1% FBS, 1% ITS (insulin, transferrin, and selenium), 0.1 µM dexamethasone, 50 µM ascorbic acid, 40 µg/ml L-proline, 1% sodium pyruvate (Sigma, UK) and 10 ng/ml TGFb3 (transforming growth factor-b3) (PeproTech, UK)). hMSC differentiation progressed over 3 weeks with twice weekly media changes followed by PBS washes and fixation with 10% neutral-buffered formalin before being analyzed with specific cytological stains: Alizarin red for osteogenic, Oil Red O for adipogenic and Alcian blue for chondrogenic differentiation (Sigma, UK).

Transcriptome analysis

We had previously determined the impact of oxygen concentration on the hMSC transcriptome under the same conditions applied in this study except for the cells being at an earlier passage number (P0).[39] We utilized this existing dataset to determine transcriptional effects across a panel of 31 bioactive factors. Expression values derived from Fischer et al.[37] were uploaded into Array Mining (http://arraymining.net) for heatmap production. Probeset values were transferred into the template file, uploaded and standard settings applied; eBayes supervised feature selection method, maximum feature subset size of 100.

Secretome analysis

A bicinchoninic acid (BCA) assay was conducted to quantify amounts of protein present in SFCM. Matched volumes of BSA standard serial dilutions and SFCM were loaded into 96-well plates and 100 µl BCA reagent added to each well. According to manufacturer instruction, the reagent was prepared by mixing 2% (v/v) copper sulphate solution with BCA solution (Sigma, UK). The plate was incubated at 37°C for 1 h and optical density determined at 570 nm via a Synergy2 plate reader (BioTek, UK).

The Human Cytokine ELISA Plate Array (Signosis, UK) was used to determine specific changes in bioactive molecule concentration. SFCM (100 µl from AO, IH, and P) were first loaded into a manufacturer-supplied 96-well plate pre-coated with well-specific capture antibodies followed by incubation for 2 h with gentle shaking. After incubation, each sample well had an additional 100 µl diluted biotin-labelled antibody mixture added followed by a further 1 h incubation with gentle shaking. Then, samples were incubated with 100 µl diluted streptavidin-HRP conjugate for 45 min with gentle shaking. Each step was accompanied by forcibly discarding the content and four washes with diluted detergent buffer. Enzymatic reactions were then initiated via addition of a substrate, 30 min incubation at room temperature and finally reaction termination by adding the stop solution. Visible signal was detected at 450 nm via a plate reader.

ELISA was performed for IL2, IL4, IL10, tumor necrosis factor alpha (TNFa), placenta growth factor-1 (PIGF1), and VEGF (PeproTech, UK). Standard serial dilutions and SFCM in triplicate were loaded into wells pre-coated with a capture antibody specific to one of the listed cytokines and blocked for 1 h with BSA-blocking buffer. Then, the plates were incubated for 2 h with diluted detection antibody mixture followed by 30 min with diluted avidin-HRP. Each step was accompanied by forcibly discarding the contents and four rounds of washing with diluted detergent buffer. Finally, ABTS-substrate (2,2′-Azino-bis(3-ethylbenzothiazoline-6-sulfonic acid)) (Sigma, UK) was added for 5–15 min and visible signal detected at 405 nm via a plate reader.

Statistical analysis

Statistical analysis was conducted using Prism 6 (GraphPad, USA) with further analysis performed in

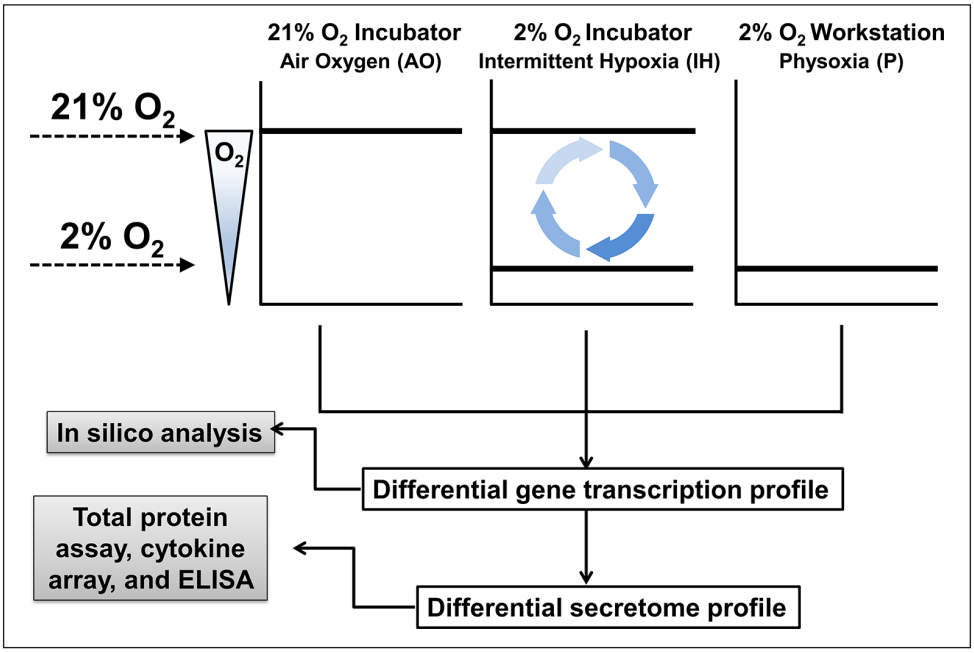

Figure 1. Experimental design for the evaluation of oxygen modulation on hMSC secretome. SFCM from hMSC cultures were collected under specified oxygen tensions and used for subsequent experimentation. The 21% O_2 incubator providing a AO environment shows no fluctuation of gas phase oxygen at the cellular level during standard incubation or processing the cells outside of the incubator. In contrast, 2% O_2 incubators provide an IH environment with fluctuations in oxygen concentration when processing cultures outside of the incubator during seeding, changing media, passaging, door opening and closing. The 2% O_2 Workstation provides a P environment characterized by steady state oxygen levels in the closed culture system. Solid lines indicate the oxygen levels present in the specific culture condition.

Microsoft Excel. A 2-sample *t*-test was used in comparative groups. A value of $p < 0.05$ was estimated to indicate statistical significance differences between groups.

Results

Validation of hMSCs

Cultures of hMSCs were maintained under specified oxygen tensions consisting of AO, IH, or P (Figure 1).

The identity of isolated hMSCs was first confirmed via trilineage differentiation and flow cytometry analysis (Figure 2). Isolated hMSCs displayed positive expression of CD73 (91.1 ± 6.8, 94.9 ± 7.6, 96.5 ± 2.2), CD90 (80.9 ± 16.0, 87.3 ± 16.4, 88.5 ± 13.7), CD105 (81.2 ± 19.0, 81.4 ± 27.0, 90.2 ± 11.5) and little or no expression of CD14 (7.0 ± 2.6, 9.1 ± 3.7, 7.5 ± 1.4), CD19 (4.4 ± 1.4, 5.6 ± 0.5, 8.6 ± 4.7), CD34 (5.1 ± 0.6, 6.2 ± 0.7, 7.8 ± 2.4), CD45 (6.0 ± 1.2, 10.1 ± 3.1, 7.9 ± 2.6), and HLADR (9.0 ± 6.4, 8.5 ± 2.9, 7.4 ± 2.1), for hMSCs maintained in AO, IH, and P, respectively (Figure 2(a)). No significant differences in expression profiles were noted between AO, IH, or P conditions. Similarly, successful differentiation into adipocytes, chondrocytes, and osteocytes upon in vitro exposure to differentiation inducing media was observed, with some variability between conditions (Figure 2(b)).

Transcriptional evaluation of selected bioactive genes

Utilizing the Human Cytokine ELISA Plate Array as a guide, we determined if there was differential expression of the associated transcripts (Table 1 and Figure 3). A reanalysis of a previously published Affymetrix Exon 1.0ST dataset of hMSCs isolated under AO, IH, and P was performed to identify significant expression changes between oxygen conditions of $p \leqslant 0.1$.[37] Significant upregulation of NGF, LEP, CCL3, SERPINE1, and TGFb1 combined with down-regulation of CSF3, IGF1, IL1A, and CXCL8 were noted in IH versus AO ($p \leqslant 0.05$). A reduced number of alterations were apparent for P versus AO where LEP, CCL2, and CCL3 displayed upregulation and IGF1 downregulation ($p \leqslant 0.05$). In addition to the previously described expression patterns, differential upregulation of FGF2, CSF3, CXCL8, CCL2, and downregulation of IFNG and TGFb1 were observed in P versus IH illustrating an immediate alteration of expression profiles between these subtly divergent conditions ($p \leqslant 0.05$). A number of reportable alterations were noted straddling the significance/non-significance boundary ($0.1 \leqslant p \geqslant 0.05$) including both upregulations; CCL2 (IH vs AO), NGF, CXCL10 (P vs IH), and downregulations CCL11, FGF2 (IH vs AO), and IL1A, CXCL8 (P vs AO) (Figure 4).

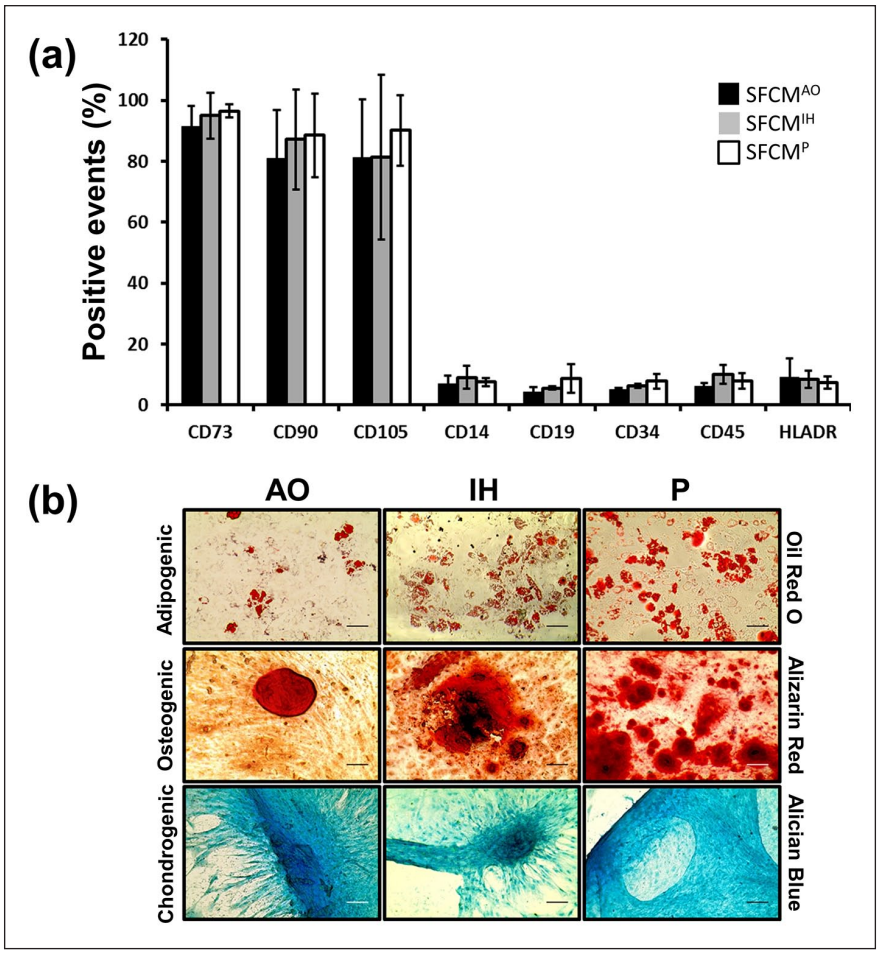

Figure 2. hMSCs immunophenotype and trilineage differentiation potential are consistent across isolation conditions. Confirmation of ISCT hMSC characterization guidelines was achieved through FACS and differentiation assays. (a) Mean positive events of CD73, CD90, CD105, CD14, CD19, CD34, CD45, and HLADR from three independent hMSC samples. AO, IH, and P are indicated by black, gray and white bars respectively. Error bars indicate ±1 SD ($n = 3$). (b) Representative images of hMSC differentiation from AO, IH, and P cultures to adipogenic, osteogenic and chondrogenic lineages. Scale bar indicates 50 μm.

Probe-specific expression values generated a supervised non-hierarchical heatmap which indicated a strong tendency for experimental conditions to cluster together more strongly than across groups. Specifically, dendogram branch length was substantially reduced for both P and IH, to a lesser extent, than that observed for AO (Figure 4).

Secretome evaluation and component determination

We next sought to determine if hMSC culture in either of AO, IH, or P would impact on the total protein concentration, and hence the secretome, found within SFCM. Strikingly we observed a normalized total protein concentration of 361.0 ± 50.0 ng/ml in $SFCM^{IH}$, 247.7 ± 49.2 ng/ml in $SFCM^{P}$ ($p < 0.05$ vs $SFCM^{IH}$), and 123.3 ± 25.2 ng/ml in $SFCM^{AO}$ ($p < 0.05$ vs $SFCM^{IH}$ and $SFCM^{P}$) (Figure 5(a)). Having identified a significant and substantial increase in IH secretome protein concentration over both P and AO, we next sought to determine the impact on individual components via the Human ELISA Cytokine Plate Array. The overall indication was that $SFCM^{IH}$ contained the highest level of each individual component tested (excepting IP10), noting that there was substantial variability across biological replicates (Figure 5(b) and Table 2)). Greater than 2-fold upregulation in $SFCM^{IH}$ and $SFCM^{P}$ versus $SFCM^{AO}$ was observed for Adiponectin (2.7-fold, 2.2-fold), EGF (5.6-fold, 3.2-fold), GCSF (4.4-fold, 3.8-fold), IL2 (5.3-fold, 2.1-fold), IL17a (4.5-fold, 3.0-fold), IP10 (2.6-fold, 3.2-fold), and Rantes (47.0-fold, 6.5-fold), respectively. Upregulation of 2-fold or greater specific to $SFCM^{IH}$ versus $SFCM^{AO}$ was found for IGF1 (2.0 fold), bNGF (4.8-fold), VEGF (2.4-fold), and IL6 (2.3-fold). Substantial upregulation was also observed for $SFCM^{IH}$ versus $SFCM^{P}$ for IL4 (2.3-fold), IL2 (2.5-fold), bNGF (3.1-fold), MCP1 (2.4-fold) and Rantes (7.2-fold). Significant upregulation of bNGF, EGF, and IL6 were

Table 1. Affymetrix probeset expression values for proteins present on the human cytokine ELISA plate array.

Gene	Propset	AO		IH		P	
ID	ID	Mean	SD	Mean	SD	Mean	SD
ADIPOQ	207175_at	101.7	22.0	106.7	16.1	114.4	24.1
NGF	206814_at	277.5	92.3	460.2	132.7	407.9	42.4
EGF	206254_at	85.7	12.1	91.2	14.5	105.7	18.1
CCL11	210133_at	90.0	13.3	72.8	8.1	76.8	12.0
FGF2	204422_s_at	2634.0	496.5	2129.0	338.9	2820.0	412.9
	204421_s_at	1771.5	545.2	1343.8	430.3	1738.2	403.3
	240243_at	135.5	38.1	100.8	18.3	87.5	23.4
	220183_s_at	176.9	90.9	128.5	44.5	154.3	73.8
	230329_s_at	233.7	284.6	152.7	87.2	160.7	121.1
CSF3	207442_at	272.0	34.3	222.0	9.6	254.1	20.2
CSF2	210229_s_at	216.1	36.3	179.9	24.8	246.9	72.2
IFNG	210354_at	23.4	6.4	22.1	2.3	20.2	1.7
IGF1	209540_at	158.2	31.4	95.9	4.6	98.9	9.4
	209541_at	158.2	31.4	95.9	4.6	98.9	9.4
	209542_x_at	190.3	39.8	118.4	5.6	120.8	10.9
	211577_s_at	237.5	42.5	144.8	6.7	151.5	12.5
IL1α	208200_at	70.4	31.1	33.3	6.0	37.2	5.0
	210118_s_at	66.3	28.8	31.6	7.0	36.1	6.7
IL2	207849_at	13.0	1.1	14.8	5.4	15.0	5.7
IL4	207538_at	49.9	5.2	47.7	3.5	48.1	5.8
	207539_s_at	49.9	5.2	47.7	3.5	48.1	5.8
IL6	205207_at	2110.2	481.8	1915.0	753.6	2188.1	353.1
CXCL8	202859_x_at	3230.5	1236.8	681.2	390.0	1465.1	674.4
	211506_s_at	3888.7	1427.7	794.4	421.0	1664.2	722.7
IL10	207433_at	86.1	7.4	87.2	8.0	84.3	6.2
IL12β	1560725_at	67.4	10.4	77.4	7.4	75.1	11.8
	207160_at	109.7	29.9	95.3	19.0	101.7	12.4
IL13	207844_at	68.2	10.2	65.8	4.8	74.1	15.8
IL17α	208402_at	78.4	13.1	76.1	7.2	70.9	10.8
	216876_s_at	88.0	15.2	81.4	10.7	79.4	13.7
CXCL10	210147_at	36.3	12.1	35.1	3.0	41.6	1.5
	204533_at	40.2	8.5	31.6	6.7	30.3	7.2
LEP	207092_at	106.5	24.4	221.3	66.8	207.0	21.7
CCL2	216598_s_at	1766.0	484.9	2458.7	243.5	3465.6	294.1
CCL3	234223_at	17.6	6.8	17.1	2.6	25.2	5.8
	233210_at	18.1	1.2	21.7	5.7	24.1	9.8
	205114_s_at	84.2	18.7	121.8	27.6	104.4	10.7
SERPINE1	202627_s_at	5103.4	428.6	6118.4	177.0	5740.9	507.2
	1568765_at	2516.0	655.2	2999.4	228.9	2945.7	267.3
	202628_s_at	5615.7	427.2	6756.1	200.4	6268.7	574.2
PDGF	217112_at	123.9	11.9	104.9	10.3	111.7	14.1
	216055_at	80.8	37.3	45.1	6.4	77.5	10.7
	204200_s_at	191.3	27.4	182.1	18.6	212.9	24.0
	217430_x_at	12,848.8	978.9	12,867.7	875.7	11,953.5	1942.2
PIGF	209652_s_at	410.4	111.3	455.6	30.8	477.5	89.3
	215179_x_at	368.2	92.1	349.2	15.0	446.8	69.0
CCL5	204655_at	150.0	29.6	140.4	15.2	141.4	13.8
	1555759_a_at	150.0	29.6	140.4	15.2	141.4	13.8
RETN	1568617_a_at	143.5	22.4	140.3	11.3	150.5	9.0
	220570_at	242.3	19.2	239.8	31.0	276.5	30.0
KITLG	207029_at	79.5	39.2	79.8	26.6	89.9	17.6
	211124_s_at	70.6	34.6	67.4	23.3	77.8	13.9
TGFβ1	203084_at	628.9	202.0	1077.1	74.7	933.5	131.7
	203085_s_at	574.5	168.5	981.9	84.4	839.5	119.3
TNF	207113_s_at	83.5	8.1	91.5	11.5	83.3	8.8
VEGFα	212171_x_at	3640.1	349.7	4121.3	284.7	3745.3	519.9
	210512_s_at	5086.7	434.9	5639.4	351.2	5003.6	748.7
	211527_x_at	4733.1	471.2	5308.6	393.1	4832.6	680.9
	210513_s_at	6853.6	735.1	7375.9	517.5	6529.4	1003.3

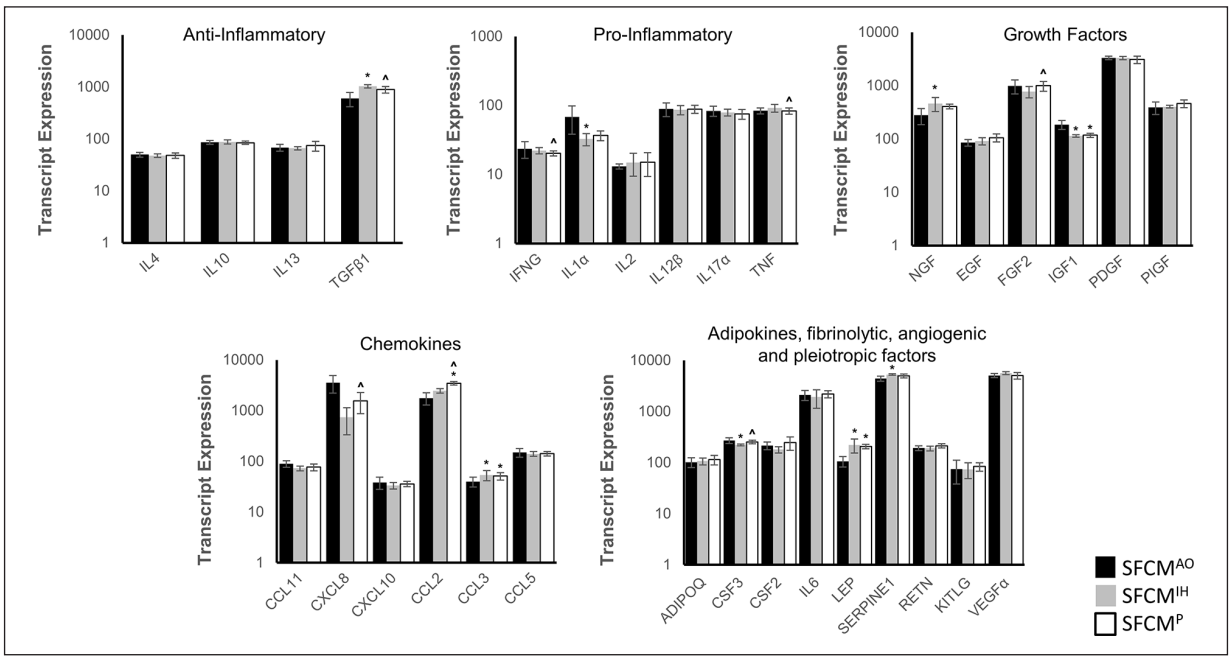

Figure 3. Bioactive panel transcript analysis across multiple hMSC samples. (a) Expression values of 31 bioactive transcripts drawn from previously published in silico analysis (Fischer et al.[37]). The average values are plotted on the *y*-axis, error bars indicate ±SD. AO, IH, and P are indicated by black, gray, and white bars respectively. *indicates $p < 0.05$ versus AO, ^ indicates $p < 0.05$ versus IH.

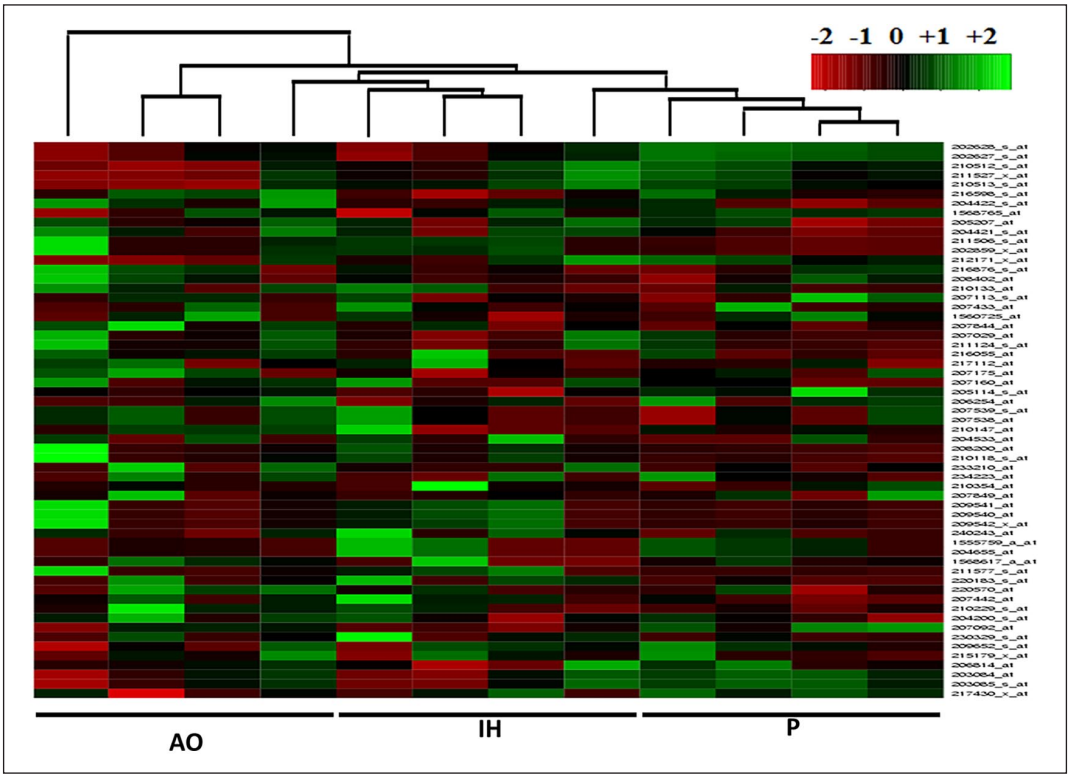

Figure 4. Heatmap generation (ArrayMining) showing specific oxygen environment clustering. Individual columns represent hMSC expression profile from within specified condition; AO, IH, or P. Labelling convention is upregulation (green), no change (black), and down-regulation (red). The dendrogram indicates unsupervised clustering across the sample dataset used to generate the heatmap and expression data.

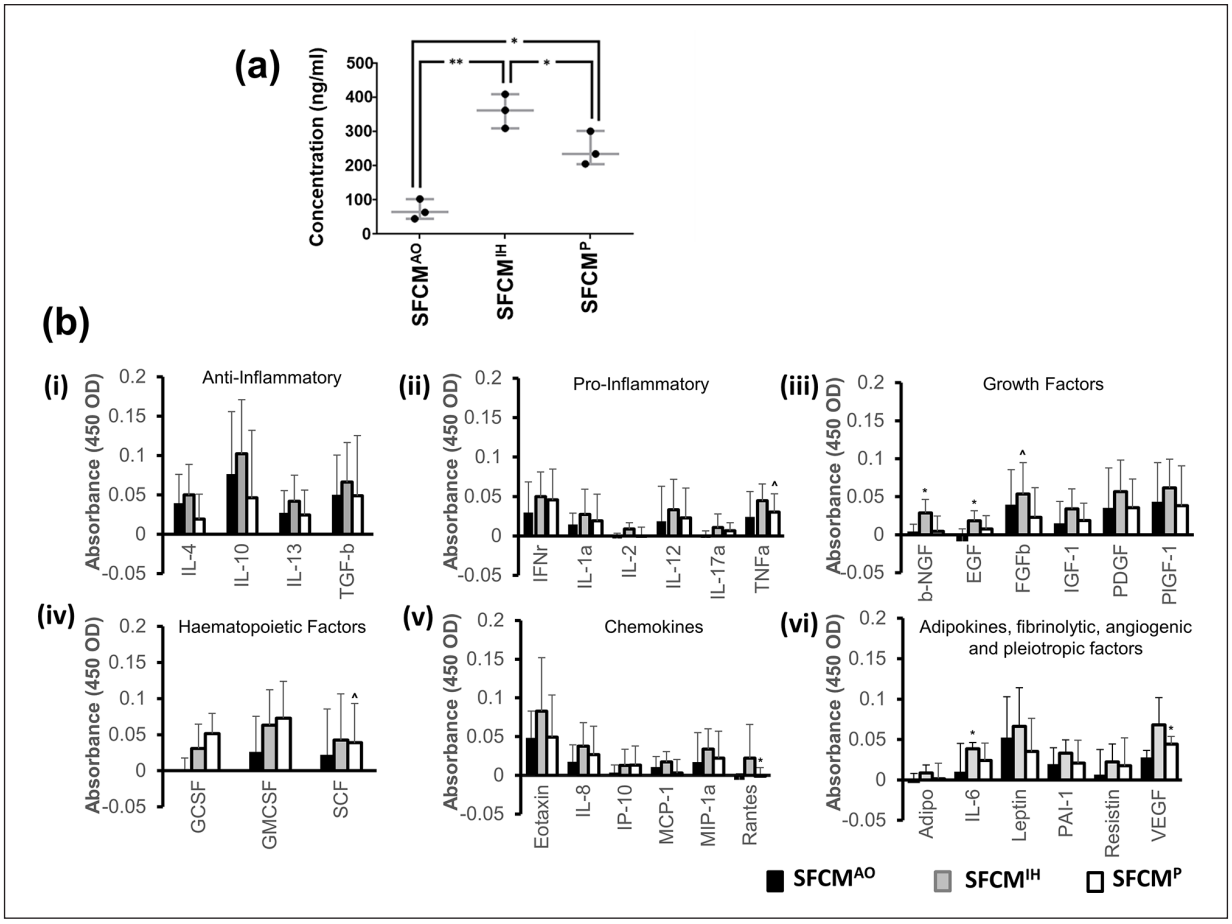

Figure 5. Proteomic assessment of hMSC secretome. (a) Total protein content of SFCM was evaluated in AO, IH, and P cultured hMSCs via the Smith assay. Protein concentration is plotted on the *y*-axis whilst oxygen environment is indicated along the *x*-axis. Data expressed as mean ± SD, *$p < 0.05$ and **$p < 0.001$ ($n = 3$). (b) Colorimetric cytokine array of SFCM expressed as mean ± SD. The 31 bioactive factors were sub-classified into nine functional groups: (i) anti-inflammatory (IL4, IL10, IL13, and TGFb), (ii) pro-inflammatory (TNFa, IFNr, IL1a, IL2, IL12, and IL17a), (iii) growth factors (EGF, IGF1, bNGF, PIGF1, PDGF, and FGFb), (iv) haematopoietic factors (GCSF, GMCSF, and SCF), (v) chemokines (MIP1a, MCP1, Rantes, Eotaxin, IL8, and IP10) and (vi) adipokines (Resistin, Leptin, and Adiponectin), fibrinolytic factor (PAI1), angiogenic factor (VEGF), pleiotropic factor (IL6). Bioactive molecule tested is indicated along the *x*-axis and colorimetric absorbance plotted on the *y*-axis. AO, IH, and P are indicated by black, gray and white bars respectively. *indicates $p < 0.05$ versus AO, ^ indicates $p < 0.05$ versus IH ($n = 4$).

noted in $SFCM^{IH}$ versus $SFCM^{AO}$ and Rantes and VEGF for $SFCM^{P}$ versus $SFCM^{AO}$ ($p < 0.05$). We also observed significant upregulation of FGFb, SCF, and TNFa in $SFCM^{IH}$ versus $SFCM^{P}$ ($p < 0.05$). As stated previously, we encountered substantial variation between samples masking outright significance in a number of instances. These included upregulation of IGF1, IL2, MIP1a, PAI1, Resistin, TNFa, and VEGF in $SFCM^{IH}$ versus $SFCM^{AO}$ and IL6 in $SFCM^{P}$ versus $SFCM^{AO}$ ($p < 0.1$). Similarly, we noted substantial, but non-significant, increases for GMCSF, IGF1, and IL2 in $SFCM^{IH}$ versus $SFCM^{P}$ ($p < 0.1$).

Numerous alterations in protein composition were observed between condition-specific SFCM where some achieved significance levels. It remained to be determined if these changes were reflected in quantitative ELISA-based assays. We selected six proteins to explore in more detail including those where significant differences were achieved (TNFa, VEGF), were marginal (IL2) and were absent (IL4, IL10, and PIGF1) (Figure 6 and Table 2). Similar to earlier observations, we again noted significantly increased VEGF ($SFCM^{IH}$ and $SFCM^{P}$ versus $SFCM^{AO}$) ($p < 0.05$) and TNFa ($SFCM^{IH}$ versus $SFCM^{P}$ and $SFCM^{AO}$) ($p < 0.001$). Increased sensitivity revealed elevated IL2 ($SFCM^{IH}$ versus $SFCM^{P}$) ($p < 0.05$), decreased IL4 and IL10 ($SFCM^{P}$ versus $SFCM^{IH}$ and $SFCM^{AO}$) ($p < 0.05$), and increased PIGF-1 ($SFCM^{IH}$ versus $SFCM^{AO}$) ($p < 0.05$).

Finally, we sought to establish the overall profile of SFCM as attributable to individual classes of activity (Figure 7). Drawing on the 31 bioactive factors previously evaluated these were sub-classified into 9 functional groups: anti-inflammatory (IL4, IL10, IL13, and TGFb), pro-inflammatory (TNFa, IFNr, IL1a, IL2, IL12, and

Table 2. Mean absorbance (450 OD) values from Human Cytokine ELISA Plate array across AO, IH, and P. Protein identification drawn from manufacturer's plate array composition details.

Protein ID	Gene	AO		IH		P	
	ID	Mean	SD	Mean	SD	Mean	SD
Adipo	ADIPOQ	0.0E+00	1.2E-02	8.5E-03	9.8E-03	1.5E-03	1.9E-02
βNGF	NGF	4.3E-03	9.7E-03	2.9E-02	1.8E-02	4.5E-03	2.0E-02
EGF	EGF	7.5E-04	6.4E-03	1.8E-02	1.3E-02	7.5E-03	1.7E-02
Eotaxin	CCL11	4.9E-02	3.5E-02	8.3E-02	6.9E-02	5.0E-02	5.4E-02
FGFβ	FGF2	4.0E-02	4.6E-02	5.4E-02	4.1E-02	2.3E-02	3.9E-02
GCSF	CSF3	5.0E-04	1.7E-02	2.6E-02	3.4E-02	2.2E-02	2.8E-02
GMCSF	CSF2	3.1E-02	4.9E-02	6.3E-02	4.9E-02	4.3E-02	5.1E-02
IFNr	IFNG	3.0E-02	3.9E-02	5.0E-02	3.1E-02	4.6E-02	3.9E-02
IGF1	IGF1	1.5E-02	2.9E-02	3.4E-02	2.6E-02	1.9E-02	2.3E-02
IL1α	IL1A	1.5E-02	1.4E-02	2.7E-02	3.2E-02	1.9E-02	3.4E-02
IL2	IL2	7.5E-05	2.2E-03	9.0E-03	7.7E-03	3.0E-06	2.4E-03
IL4	IL4	4.0E-02	3.7E-02	5.0E-02	3.9E-02	1.9E-02	3.2E-02
IL6	IL6	1.0E-02	3.5E-02	3.9E-02	7.6E-03	2.4E-02	2.1E-02
IL8	CXCL8	1.8E-02	2.2E-02	3.8E-02	3.0E-02	2.7E-02	3.7E-02
IL10	IL10	7.7E-02	7.9E-02	1.0E-01	6.9E-02	4.6E-02	8.6E-02
IL13	IL12B	2.7E-02	2.8E-02	4.2E-02	3.3E-02	2.5E-02	3.2E-02
IL12	IL13	1.9E-02	4.4E-02	3.3E-02	3.9E-02	2.3E-02	3.8E-02
IL17α	IL17A	7.8E-04	2.7E-03	1.1E-02	1.7E-02	6.8E-03	1.0E-02
IP10	CXCL10	3.5E-03	9.9E-03	1.3E-02	2.1E-02	1.3E-02	2.5E-02
Leptin	LEP	5.2E-02	5.1E-02	6.6E-02	4.8E-02	3.5E-02	4.1E-02
MCP1	CCL2	1.1E-02	1.4E-02	1.7E-02	1.4E-02	3.0E-03	1.7E-02
MIP1α	CCL3	1.7E-02	3.8E-02	3.4E-02	2.6E-02	2.2E-02	3.5E-02
PAI1	SERPINE1	2.0E-02	2.0E-02	3.3E-02	1.6E-02	2.1E-02	2.8E-02
PDGF	PDGF	3.5E-02	5.2E-02	5.7E-02	4.1E-02	3.6E-02	3.8E-02
PlGF1	PlGF	4.4E-02	5.1E-02	6.2E-02	3.8E-02	3.8E-02	5.2E-02
Rantes	CCL5	7.5E-05	4.5E-02	2.2E-02	4.3E-02	1.3E-04	1.5E-03
Resistin	RETN	6.8E-03	3.1E-02	2.2E-02	2.2E-02	1.8E-02	3.5E-02
SCF	KITLG	5.2E-02	6.3E-02	7.3E-02	6.4E-02	3.9E-02	5.4E-02
TGFβ	TGFB1	5.0E-02	5.0E-02	6.6E-02	5.0E-02	4.9E-02	7.6E-02
TNFα	TNF	2.4E-02	3.2E-02	4.5E-02	2.2E-02	3.0E-02	2.3E-02
VEGF	VEGFA	2.8E-02	8.7E-03	6.8E-02	3.4E-02	4.4E-02	9.5E-03

IL17a), growth factors (EGF, IGF1, bNGF, PIGF1, PDGF, and FGFb), hematopoietic factors (GCSF, GMCSF, and SCF), chemokines (MIP1a, MCP1, Rantes, Eotaxin, IL8, and IP10), adipokines (Resistin, Leptin, and Adiponectin), fibrinolytic factor (PAI1), angiogenic factor (VEGF), and pleiotropic factor (IL6). The overall abundance of growth factors, hematopoietic factors, adipokines, angiogenic, and fibrinolytic factors remained unchanged across the three oxygen conditions. $SFCM^{AO}$ displayed an 8% increase in abundance of anti-inflammatory cytokines when compared to $SFCM^{IH}$ and $SFCM^{P}$. Conversely, pro-inflammatory cytokines in $SFCM^{P}$ were 4%–5% higher than in all other conditions and chemokines and pleiotropic factors 2%–3% lower in $SFCM^{AO}$ than in other conditions.

Discussion

The role of stem cells and their products in regenerative medicine therapeutics require mechanistic understanding to support increased delivery via hospital-based models. Previous studies have delineated key transcription and behavioral changes in MSCs resulting from subtle biophysical alterations, including those likely to arise following on from transplantation and delivery.[35,37,38] We have added to that body of knowledge in this study by demonstrating that the secretome of in vitro-cultured bone marrow-derived hMSCs varies significantly in an oxygen-dependent manner. Reducing oxygen levels to reflect either physoxia or pathological hypoxia results in a potentiation of secreted biomolecules when compared to air-cultured hMSCs. Defining the secretome of hMSCs under biophysical conditions resembling the milieu immediately following transplantation is an important first step in accurately identifying molecules responsible for therapeutic effects and/or the potency of SFCM as a biotherapy.

Three bone marrow aspirates (BMAs) from both male and female donors spanning 20–36 years of age were used

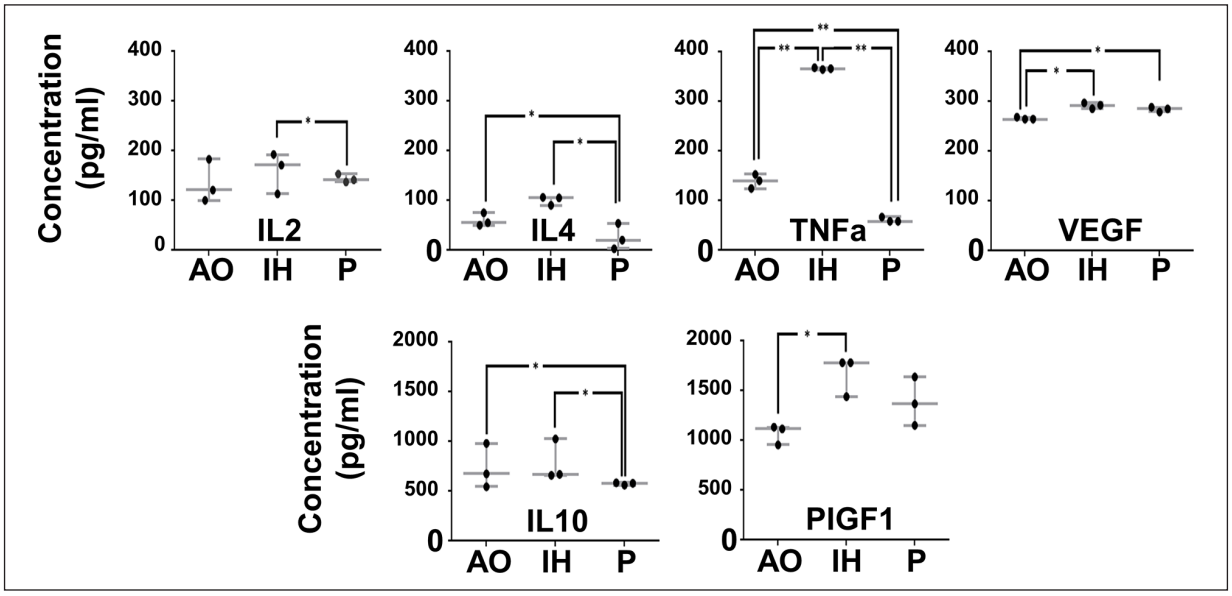

Figure 6. hMSC secretome composition is modified by oxygen environment. ELISA assays were performed to quantify changes in IL2, IL4, IL10, TNFa, PIGF1, and VEGF which were found to be significantly different between AO, IH and P in the cytokine array analysis. Protein concentration is plotted on the y-axis whilst oxygen environment is indicated along the x-axis. Data expressed as mean ± SD, *$p < 0.05$ and **$p < 0.001$ ($n = 3$).

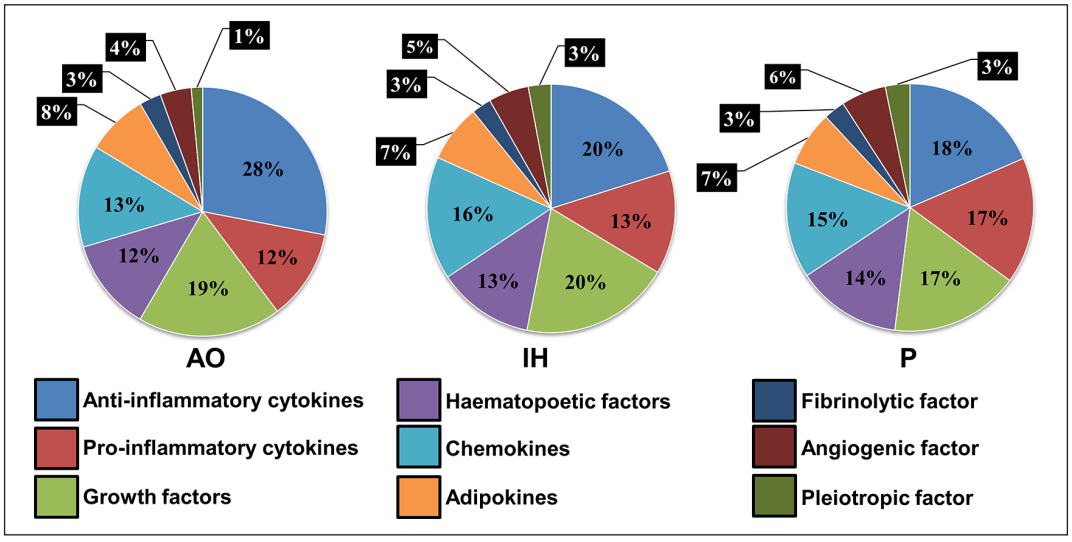

Figure 7. Functional classification of SFCM components. Bioactive factors previously evaluated were subclassified into nine functional groups across the three oxygen conditions; anti-inflammatory, pro-inflammatory, growth factors, hematopoietic factors, chemokines, adipokines, fibrinolytic factor, angiogenic factor, and pleiotropic factor. The percentage breakdown of each functional class in each oxygen culture environment is plotted as a pie chart.

in this study to isolate hMSCs, and subsequently produce SFCM which was assessed for differences in secretome composition resulting from the culture under different oxygen tensions. The analyzed SFCM was produced from hMSCs at P1 while the transcriptome dataset was produced from data recorded from previous work using hMSCs at P0. Time taken for hMSC isolation from BMA plating, expansion, passaging and reaching confluence at P1 was 28–29 days and was consistent between the three oxygen concentrations. It is important to note the caveats associated with the use of BMAs from donors of different gender and age and the implications this could have including the comparisons with other studies. The influence of donor age on hMSC gene expression profiles, morphology and growth characteristics have previously been demonstrated.[42–45] Another consideration when drawing parallels

with other published studies is the differing oxygen concentrations used to represent physoxia, 2% in this study, and the implications this has in potentially altering the secretome composition. The study of a larger number of BMAs according to a power analysis from donors spanning a broader age range as well as male and female donors would allow for the identification of more subtle alterations in expression and secretome values, which were seen to stagger the boundary of significance in this study.

Physoxia is significantly lower than inhaled air (21% O_2) which declines as it passes from the lung to the tissues; ranging between 0.1% and 9% with an average of 2% O_2.[31–33,35] In this study, 2% O_2 was rationalized as a physiologically relevant oxygen tension with which to culture hMSCs due to the $p0_2$ of in vivo environments ranging between 0.1% and 9% and more specifically sinusoidal bone marrow which was showed to have an average value of 2.7%.[34] Assessment of any differences in the MSC secretome at different levels of physoxia, for instance modelling exposure linked to maximal diffusion co-efficient would allow a deeper understanding and allow for more in depth comparisons with other published studies.

A number of previous studies have analyzed the serum-free in vitro secretome of hMSCs. Biomolecules identified in the secretome of air-cultured hMSCs have included anti-inflammatory (IL4, IL10, IL13, and TGFb),[6,46] pro-inflammatory (IL2, IL12, IFNr, TNFa, and IL1a),[6,47] chemokines (Rantes, MCP1, IL8, and MIP1b),[6,48] hemopoietic (G-CSF, and GM-CSF),[6] and pleiotropic factors (IL6).[6,15] Substantial overlap and significant discrepancy is a key feature of hMSC secretome defining studies. For instance, while IL1b, IL15, IL1a, Rantes, VEGF-A, FGFb, and HGF were noted as air-cultured hMSC secretome components, after 14-days incubation, (in addition to IL8, MCP-1 and IL6, and RANTES) a range of previously described components were not (IL2, IL4, IL10, IL12, IL13, TNFa, MIP1b, G-CSF, or GM-CSF).[49] While shorter-term serum-free culture over an initial 24 h resulted in detection of Angiogenin, GRO, IGF1 and TIMP1 (and confirmation of IL6, RANTES, TGFb1, and VEGF), notable was the absence of FGFb, IFNg, IL8 with EGF, CXCL5, PDGF, PLGF, and TPO.[13] In broad agreement with previous studies, we also noted an air-cultured hMSC secretome contained FGFb, GM-CSF, IFNr, IL1a, IL4, IL8, IL10, IL12, MCP1, TGFb, TNFa, and VEGF which may form the basis of a minimal air-cultured hMSC secretome.[6,46–49] Similarly, IL2, IL6, IL13, MIP1a, and RANTES lay below a detectable threshold in our experimentation.

Reduced oxygen culture (~1% O_2) is described as a positive mediator of chemotactic and growth factor upregulation in the hMSC secretome.[50,51] Comparison of the hMSC secretome produced in air oxygen (21% O_2) to virtual anoxia (0.1% O_2) and physoxia (5% O_2) oxygen tension environments experienced during in vivo-based therapies identified significant differences in component profiles. Paracrine expression levels of IL8, MCP1, RANTES, VEGF-A, and VEGF-C were enhanced under 0.1% O_2 exposure resulting in a unique hMSC secretome profile when compared to both 5% and 21% O_2.[49] Additional significant upregulations at day 14 included IL1b, IL6, IL1, Rantes, IL15, FGFb, and HGF in 5% O_2 and 21% O_2 but not in 0.1 % O_2. Taken together, this indicates the likely divergence of hMSC secretome profiles in an oxygen-dependant manner. Similarly, we noted in this study that alternate oxygen environments significantly altered both secretome composition and component concentrations. Differences were apparent in our observations including significant upregulation of IL6 in $SFCM^{IH}$ versus $SFCM^{AO}$, RANTES in $SFCM^{P}$ versus $SFCM^{AO}$ and EGF upregulation in $SFCM^{IH}$ versus $SFCM^{AO}$. In contrast to Paquet et al, our findings suggested that secretome from hMSCs maintained in reduced oxygen displayed elevated FGFb and HGF in comparison to AO cultured hMSCs.[49,52] Differences in study design parameters make further comparison difficult. However, consistent with our observations, a range of in vitro SFCM proteomic studies have revealed upregulation of bioactive factors in reduced oxygen over AO despite differences in the source of isolated MSCs; adipose[10,53,54] or bone marrow,[7,55,56] and variation in conditioning periods. For instance, transient (6 h) exposure of adipose-derived MSCs to 5% O_2 is described as promoting IL6 and TGFb secretion whilst prolonged (72 h) exposure promotes the upregulation of GCSF, MCSF, and PDGF and downregulation of EGF.[53,54] Further conflicting analysis emerges where analysis of SFCM from BMA-derived hMSCs revealed that 1%–2% O_2 substantially induced the production of some biomolecules (ADM, DKK1, FGFb, IL6, IL8, PLGF, SDF1, and VEGF) but surprisingly, not in a number of previously reported factors (IL6, VEGF, and HGF).[55,56]

It has been suggested that the application of a critical environment, pathological hypoxia, on in vitro-cultured MSCs may stimulate cellular compensatory defense mechanisms; resulting in upregulation of the secreted proteins best suited to protect the cells from harsh environments and prolong their survival.[23,53,57,58] In ischemic injury, such as coronary arterial stenosis, tissue hypoxia is accompanied by an upregulated release of growth factors e.g. bFGF and VEGF resulting in collateral angiogenesis.[23] We have noted that physoxia mitigated the synthesis and secretion of bioactive factors in comparison to intermittent hypoxia, providing a perspective on the intrinsic behavior of MSCs in their endogenous niche while exposed to a consistent physiological oxygen tension. We hypothesize that the behaviors and resultant secretome produced by hMSCs cultured in intermittent hypoxia likely underpin the in vivo paracrine behavior of MSCs. Due to the scarcity of data available for direct comparison of our study to others, it is clear that subsequent studies should be concerned with

characterizing common secretory factors produced by in vivo transplanted MSCs to those identified in our study.[59] The translation of an hMSC-based secretome into clinical application provides an opportunity for the ultimate replacement of cell-based therapeutics with a cell-free therapy, likely overcoming immunogenicity and ethical hurdles.[60] However, predictability of safety and efficacy of the cell-free product would be drawn from the presence of individual components at pre-specified concentration levels which are anticipated to be affected by a range of in vitro factors including, as we have demonstrated, oxygen culture conditions.[61] Advancements in proteomics coupled to an optimization of in vitro culture conditions will play a major role in the identification of constituent components of the hMSCs-secretome encouraging batch reproducibility, minimizing variability, and permitting appropriate dispensation for future applications.

Conclusion

The efficacy of hMSCs as a therapy may be linked to released bioactive factors; such as cytokines, whose secretion is either constitutive or regulated. Priming hMSC with alternate in vitro stimuli has the potential to modulate the quantity and composition of components released, resulting in improved or modulated potency of the cell-based or cell-free biotherapy. hMSCs exposed to intermittent hypoxia and physoxia have reprogrammed their intracellular machinery to synthesize/secrete more protein-based constituents with the potential to enhance the potency of the cell-free biotherapy. In turn, this has the potential to help overcome translational drawbacks associated with cell-based therapy including poor homing potential, limited cell survival, and uncertain mechanisms of action.

Declaration of conflicting interests

The author(s) declared no potential conflicts of interest with respect to the research, authorship, and/or publication of this article.

Funding

The author(s) disclosed receipt of the following financial support for the research, authorship, and/or publication of this article: Financial support provided by Ministry of Higher Education and Scientific Research, Iraq (S1443) and the Guy Hilton Asthma Trust.

ORCID iD

Matthew T Shephard https://orcid.org/0000-0003-4625-915X

References

1. Zhao Q, Ren H and Han Z. Mesenchymal stem cells: immunomodulatory capability and clinical potential in immune diseases. *J Cell Immunother* 2016; 2(1): 3–20.
2. Németh K, Leelahavanichkul A, Yuen PS, et al. Bone marrow stromal cells attenuate sepsis via prostaglandin E2—dependent reprogramming of host macrophages to increase their interleukin-10 production. *Nat Med* 2008; 15(1): 42–49.
3. Vizoso FJ, Eiro N, Cid S, et al. Mesenchymal stem cell secretome: toward cell-free therapeutic strategies in regenerative medicine. *Int J Mol Sci* 2017; 18(9): 1852.
4. Orlic D, Kajstura J, Chimenti S, et al. Bone marrow cells regenerate infarcted myocardium. *Nature* 2001; 410(6829): 701–705.
5. Plotnikov EY, Khryapenkova TG, Vasileva AK, et al. Cell-to-cell cross-talk between mesenchymal stem cells and cardiomyocytes in co-culture. *J Cell Mol Med* 2008; 12(5a): 1622–1631.
6. Kupcova Skalnikova H. Proteomic techniques for characterisation of mesenchymal stem cell secretome. *Biochimie* 2013; 95(12): 2196–2211.
7. Hu X, Wu R, Shehadeh LA, et al. Severe hypoxia exerts parallel and cell-specific regulation of gene expression and alternative splicing in human mesenchymal stem cells. *BMC Genomics* 2014; 15: 303.
8. Martin-Rendon E, Hale SJ, Ryan D, et al. Transcriptional profiling of human cord blood CD133+ and cultured bone marrow mesenchymal stem cells in response to hypoxia. *Stem Cells* 2007; 25(4): 1003–1012.
9. Han Y, Ren J, Bai Y, et al. Exosomes from hypoxia-treated human adipose-derived mesenchymal stem cells enhance angiogenesis through VEGF/VEGF-R. *Int J Biochem Cell Biol* 2019; 109: 59–68.
10. Sagaradze G, Grigorieva O, Nimiritsky P, et al. Conditioned medium from human mesenchymal stromal cells: towards the clinical translation. *Int J Mol Sci* 2019; 20(7): 1656.
11. Liu CH and Hwang SM. Cytokine interactions in mesenchymal stem cells from cord blood. *Cytokine* 2005; 32(6): 270–279.
12. Ribeiro CA, Fraga JS, Grãos M, et al. The secretome of stem cells isolated from the adipose tissue and wharton jelly acts differently on central nervous system derived cell populations. *Stem Cell Res Ther* 2012; 3(3): 18–18.
13. Oskowitz A, McFerrin H, Gutschow M, et al. Serum-deprived human multipotent mesenchymal stromal cells (MSCs) are highly angiogenic. *Stem Cell Res* 2011; 6(3): 215–225.
14. Kim HS, Choi DY, Yun SJ, et al. Proteomic analysis of microvesicles derived from human mesenchymal stem cells. *J Proteome Res* 2012; 11(2): 839–849.
15. Potian JA, Aviv H, Ponzio NM, et al. Veto-like activity of mesenchymal stem cells: functional discrimination between cellular responses to alloantigens and recall antigens. *J Immunol* 2003; 171(7): 3426–3434.
16. Sze SK, de Kleijn DP, Lai RC, et al. Elucidating the secretion proteome of human embryonic stem cell-derived mesenchymal stem cells. *Mol Cell Proteomics* 2007; 6(10): 1680–1689.
17. Bhang SH, Lee S, Shin JY, et al. Efficacious and clinically relevant conditioned medium of human adipose-derived stem cells for therapeutic angiogenesis. *Mol Ther* 2014; 22(4): 862–872.
18. Chen J, Li Y, Hao H, et al. Mesenchymal stem cell conditioned medium promotes proliferation and migration of alveolar epithelial cells under septic conditions in vitro via the JNK-P38 signaling pathway. *Cell Physiol Biochem* 2015; 37(5): 1830–1846.
19. Walter MN, Wright KT, Fuller HR, et al. Mesenchymal stem cell-conditioned medium accelerates skin wound

healing: an in vitro study of fibroblast and keratinocyte scratch assays. *Exp Cell Res* 2010; 316(7): 1271–1281.
20. Saheli M, Bayat M, Ganji R, et al. Human mesenchymal stem cells-conditioned medium improves diabetic wound healing mainly through modulating fibroblast behaviors. *Arch Dermatol Res* 2020; 312(5): 325–336.
21. Jain R, Vakil D, Cunningham C, et al. Human mesenchymal stem cells conditioned media promotes the wound healing process - an in vitro study. *J Stem Cell Ther Transplant* 2019; 3: 028–030.
22. Chen L, Tredget EE, Wu PY, et al. Paracrine factors of mesenchymal stem cells recruit macrophages and endothelial lineage cells and enhance wound healing. *PLoS One* 2008; 3(4): e1886.
23. Kinnaird T, Stabile E, Burnett MS, et al. Local delivery of marrow-derived stromal cells augments collateral perfusion through paracrine mechanisms. *Circulation* 2004; 109(12): 1543–1549.
24. van Poll D, Parekkadan B, Cho CH, et al. Mesenchymal stem cell-derived molecules directly modulate hepatocellular death and regeneration in vitro and in vivo. *Hepatology* 2008; 47(5): 1634–1643.
25. Dreixler JC, Poston JN, Balyasnikova I, et al. Delayed administration of bone marrow mesenchymal stem cell conditioned medium significantly improves outcome after retinal ischemia in rats. *Investig Ophthalmol Vis Sci* 2014; 55(6): 3785–6323.
26. Jiang RH, Wu CJ, Xu XQ, et al. Hypoxic conditioned medium derived from bone marrow mesenchymal stromal cells protects against ischemic stroke in rats. *J Cell Physiol* 2019; 234(2): 1354–1368.
27. Das R, Jahr H, van Osch GJ, et al. The role of hypoxia in bone marrow-derived mesenchymal stem cells: considerations for regenerative medicine approaches. *Tissue Eng Part B Rev* 2010; 16: 159–168.
28. Choi JR, et al. Hypoxia promotes growth and viability of human adipose-derived stem cells with increased growth factors secretion. *J Asian Sci Res* 2014; 4(7): 328–338.
29. Yoshida Y, Takahashi K, Okita K, et al. Hypoxia enhances the generation of induced pluripotent stem cells. *Cell Stem Cell* 2009; 5(3): 237–241.
30. Lönne M, Lavrentieva A, Walter JG, et al. Analysis of oxygen-dependent cytokine expression in human mesenchymal stem cells derived from umbilical cord. *Cell Tissue Res* 2013; 353(1): 117–122.
31. Crisan M, Yap S, Casteilla L, et al. A perivascular origin for mesenchymal stem cells in multiple human organs. *Cell Stem Cell* 2008; 3(3): 301–313.
32. Zannettino AC, Paton S, Arthur A, et al. Multipotential human adipose-derived stromal stem cells exhibit a perivascular phenotype in vitro and in vivo. *J Cell Physiol* 2008; 214(2): 413–421.
33. Eliasson P and Jönsson JI. The hematopoietic stem cell niche: low in oxygen but a nice place to be. *J Cell Physiol* 2010; 222(1): 17–22.
34. Spencer JA, Ferraro F, Roussakis E, et al. Direct measurement of local oxygen concentration in the bone marrow of live animals. *Nature* 2014; 508: 269–273.
35. Haque N, Rahman MT, Abu Kasim NH, et al. Hypoxic culture conditions as a solution for mesenchymal stem cell based regenerative therapy. *Sci World J* 2013; 2013: 1–12.
36. Pattappa G, Schewior R, Hofmeister I, et al. Physioxia has a beneficial effect on cartilage matrix production in Interleukin-1 beta-inhibited Mesenchymal stem cell chondrogenesis. *Cells* 2019; 8: 936.
37. Fischer UM, Harting MT, Jimenez F, et al. Pulmonary passage is a major obstacle for intravenous stem cell delivery: the pulmonary first-pass effect. *Stem Cells Dev* 2009; 18(5): 683–692.
38. Rochefort GY, Vaudin P, Bonnet N, et al. Influence of hypoxia on the domiciliation of mesenchymal stem cells after infusion into rats: possibilities of targeting pulmonary artery remodeling via cells therapies? *Respir Res* 2005; 6(1): 125.
39. Kay AG, Dale TP, Akram KM, et al. BMP2 repression and optimized culture conditions promote human bone marrow-derived mesenchymal stem cell isolation. *Regen Med* 2015; 10(2): 109–125.
40. Chou KJ, Hsu CY, Huang CW, et al. Secretome of hypoxic endothelial cells stimulates bone marrow-derived mesenchymal stem cells to enhance alternative activation of macrophages. *Int J Mol Sci* 2020; 21(12): 4409.
41. Alijani N, Johari B, Moradi M, et al. A review on transcriptional regulation responses to hypoxia in mesenchymal stem cells. *Cell Biol Int* 2019; 44(1): 14–26.
42. Zarychta-Wiśniewska W, Burdzińska A, Zielniok K, et al. The influence of cell source and donor age on the tenogenic potential and chemokine secretion of human mesenchymal stromal cells. *Stem Cells Int* 2019; 2019: 1613701.
43. Siegel G, Kluba T, Hermanutz-Klein U, et al. Phenotype, donor age and gender affect function of human bone marrow-derived mesenchymal stromal cells. *BMC Med* 2013; 11: 146.
44. Zaim M, Karaman S, Cetin G, et al. Donor age and long-term culture affect differentiation and proliferation of human bone marrow mesenchymal stem cells. *Ann Hematol* 2012; 91: 1175–1186.
45. Ganguly P, El-Jawhari JJ, Giannoudis PV, et al. Age-related changes in bone marrow mesenchymal stromal cells: a potential impact on osteoporosis and osteoarthritis development. *Cell Transplant* 2017; 26: 1520–1529.
46. Sterclova M, Matej R, Mandakova P, et al. Role of interleukin 4 and its receptor in clinical presentation of chronic extrinsic allergic alveolitis: a pilot study. *Multidiscip Respir Med* 2013; 8(1): 35.
47. Jin W and Dong C. IL-17 cytokines in immunity and inflammation. *Emerg Microbes Infect* 2013; 2(9): e60.
48. Koch AE, Kunkel SL, Harlow LA, et al. Macrophage inflammatory protein-1 alpha. A novel chemotactic cytokine for macrophages in rheumatoid arthritis. *J Clin Investig* 1994; 93(3): 921–928.
49. Paquet J, Deschepper M, Moya A, et al. Oxygen tension regulates human mesenchymal stem cell paracrine functions. *Stem Cells Transl Med* 2015; 4(7): 809–821.
50. Hung SP, Ho JH, Shih YR, et al. Hypoxia promotes proliferation and osteogenic differentiation potentials of human mesenchymal stem cells. *J Orthop Res* 2012; 30(2): 260–266.
51. Quade M, Münch P, Lode A, et al. The secretome of hypoxia conditioned hMSC loaded in a central depot induces chemotaxis and angiogenesis in a biomimetic mineralized collagen bone replacement material. *Adv Healthc Mater* 2020; 9(2): 1901426.

52. Chang CP, Chio CC, Cheong CU, et al. Hypoxic preconditioning enhances the therapeutic potential of the secretome from cultured human mesenchymal stem cells in experimental traumatic brain injury. *Clin Sci* 2013; 124(3): 165–176.
53. An HY, Shin HS, Choi JS, et al. Adipose mesenchymal stem cell secretome modulated in hypoxia for remodeling of radiation-induced salivary gland damage. *PLoS One* 2015; 10(11): e0141862.
54. Park BS, Kim WS, Choi JS, et al. Hair growth stimulated by conditioned medium of adipose-derived stem cells is enhanced by hypoxia: evidence of increased growth factor secretion. *Biomed Res* 2010; 31(1): 27–34.
55. Bakondi B, Shimada IS, Perry A, et al. CD133 identifies a human bone marrow stem/progenitor cell sub-population with a repertoire of secreted factors that protect against stroke. *Mol Ther* 2009; 17(11): 1938–1947.
56. Chen L, Xu Y, Zhao J, et al. Conditioned medium from hypoxic bone marrow-derived mesenchymal stem cells enhances wound healing in mice. *PLoS One* 2014; 9(4): e96161.
57. Tsai CC, et al. Benefits of hypoxic culture on bone marrow multipotent stromal cells. *Am J Blood Res* 2012; 2(3): 148–159.
58. Cunningham CJ, Redondo-Castro E and Allan SM. The therapeutic potential of the mesenchymal stem cell secretome in ischaemic stroke. *J Cereb Blood Flow Metab* 2018; 38(8): 1276–1292.
59. Brown KJ, Formolo CA, Seol H, et al. Advances in the proteomic investigation of the cell secretome. *Expert Rev Proteomics* 2012; 9(3): 337–345.
60. Amariglio N, Hirshberg A, Scheithauer BW, et al. Donor-derived brain tumor following neural stem cell transplantation in an ataxia telangiectasia patient. *PLoS Med* 2009; 6(2): e1000029.
61. Pittenger MF, Discher DE, Péault BM, et al. Mesenchymal stem cell perspective: cell biology to clinical progress. *Regen Med* 2019; 4(1): 22.